Supporting Information

# Degradable polymers with adjustable thermoresponsiveness based on multicomponent polymerization and molecular recognition

Yue Zhang*, Shasha Liu, Changlan Xu

**Materials.** Poly(ethylene glycol) (PEG, $M_n$ = 600, 1000, 1500, 2000, and 4000 Da, J&K Scientific), N, N'-dicyclohexyl carbodiimide (DCC, Guo Yao Chemical Company, 98%), 4-(dimethylamino)-pyridine (DMAP, Alfa Aesar, 99%), 4-formylbenzoic acid (Heowns, 99%), 3, 3'-dithiodipropionic acid (Aladdin, 99%), β-cyclodextrin sulfobutyl ethers sodium salts (SBE-CD, Aladdin, 98%), mono-(6-amino-6-deoxy)-β-cyclodextrin (CD-$NH_2$, Zhiyuan Biotechnology Co., Ltd., ≥99%), (2-hydroxy-3-N, N, N-trimethylamino) propyl-β-cyclodextrin chloride (HTMAP-CD, Zhiyuan Biotechnology Co., Ltd., 99%), sodium sulfate anhydrous (AR), sodium carbonate anhydrous (AR), sodium chloride (AR), sodium thiocyanate (Macklin, 99%), and sodium iodide (Shanghai Shaoyuan Co.Ltd., 99%) were used as received. All solvents were distilled for purification before use.

**Characterization:** $^1$H NMR and $^{13}$C NMR measurements were carried out on a 400 MHz Varian UNITY-plus NMR spectrometer. And the 2D $^1$H NOESY NMR measurements were performed on a 400 MHz Bruker Advance III NMR spectrometer. The $M_n$ and the dispersity were measured by a Hitachi size exclusion chromatography (SEC) with DMF as the mobile phase and PMMA as the standards. The SEC was equipped with a Hitachi L-2490 refractive index detector and a Viscotek 270 dual detector. Matrix assisted laser desorption/ionization time-of-flight mass analysis (MALDI-TOF MS) were carried out on AutoflexIII LRF200-CID. The matrix used for the measurements of the polymer and the proteins are α-cyano-4-hydroxycinnamic acid and the 3, 5-dimethoxy-4-hydroxycinnamic acid. The scattering light intensity, hydrodynamic diameter ($D_h$), and polydispersity index (PDI) of the assemblies were measured by a Malvern Zetasizer Nano-ZS. Transmission electron microscopy (TEM) measurements were carried out on a Tecnai G2 F20 electron microscope with 200 kV operating voltage. The TEM specimens were prepared by

dropping the sample solution on a Formvar and carbon coated Cu grid. A solution of P(PEG1500)-1 with a concentration of 0.5 mg/mL was dropped onto a Cu grid at 40 °C. Excess solution was absorbed with filter paper and held at 40 °C for 0.5 h to dry the sample. The dried sample was first stained in a hydrazine hydrate atmosphere for 3 h, then dried in vacuum drying for 0.5 h. Finally, the dried sample was stained in $OsO_4$ for 0.5 h. For P(PEG600)-1, the sample was prepared at a temperature of 25 °C, and the rest of the steps were the same as above. Scanning electron microscopy (SEM) was measured with an FEI Apreo S LoVac electron microscope.

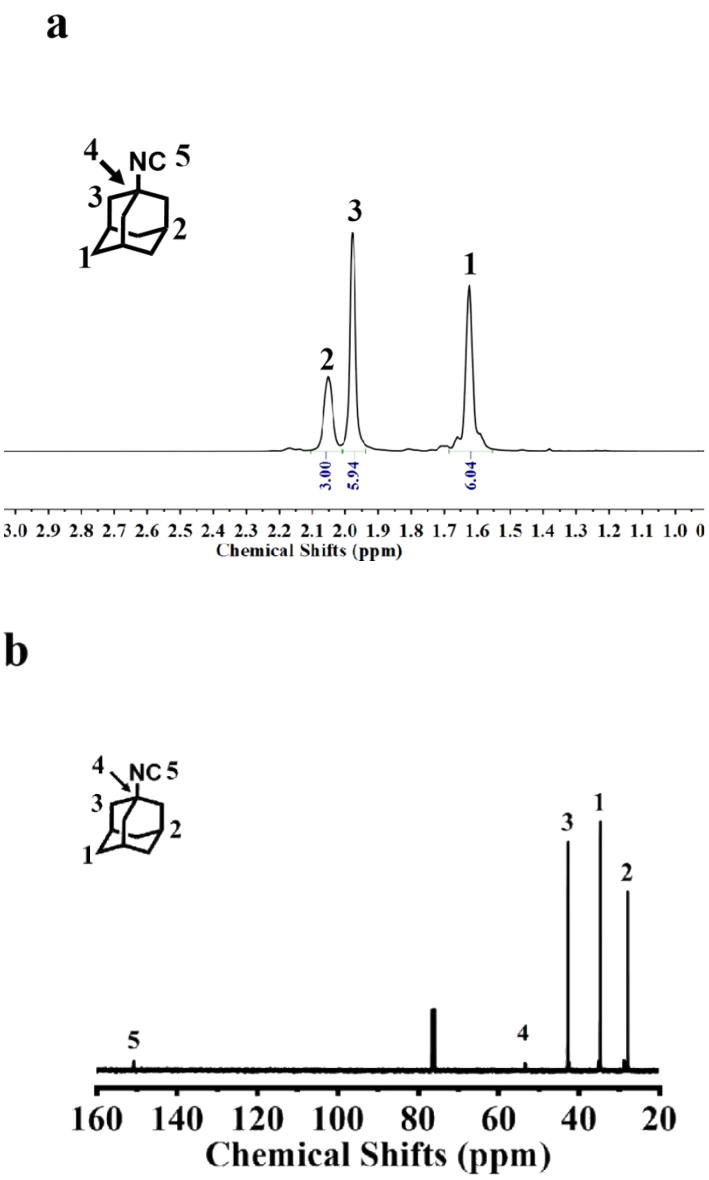


Figure S1. $^{1}H$ NMR (a) and $^{13}C$ NMR (b) spectra of the Ad-NC in $CDCl_3$.

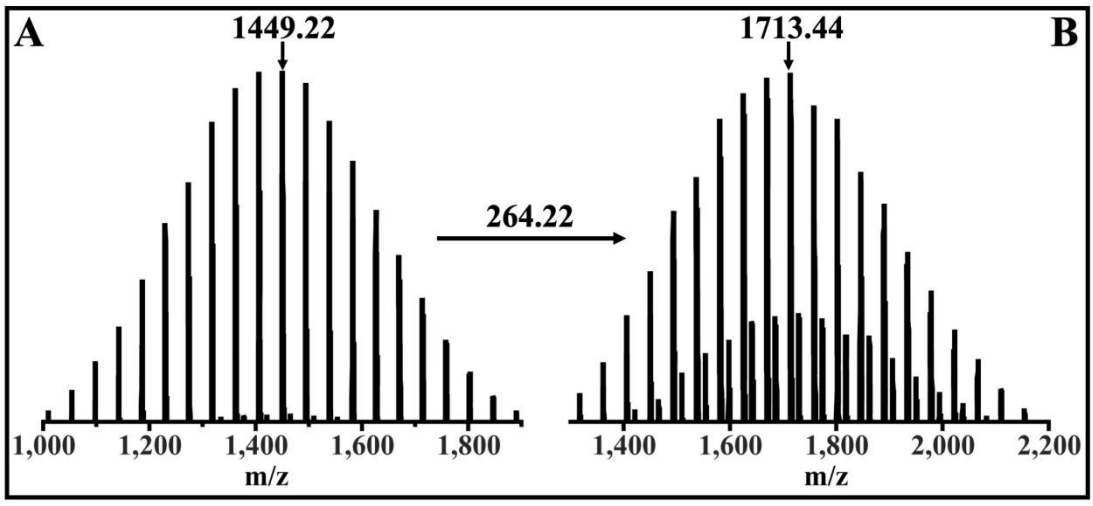


Figure S2. MALDI-TOF MS results of PEG1500 (a) and CHO-PEG1500-CHO (b).

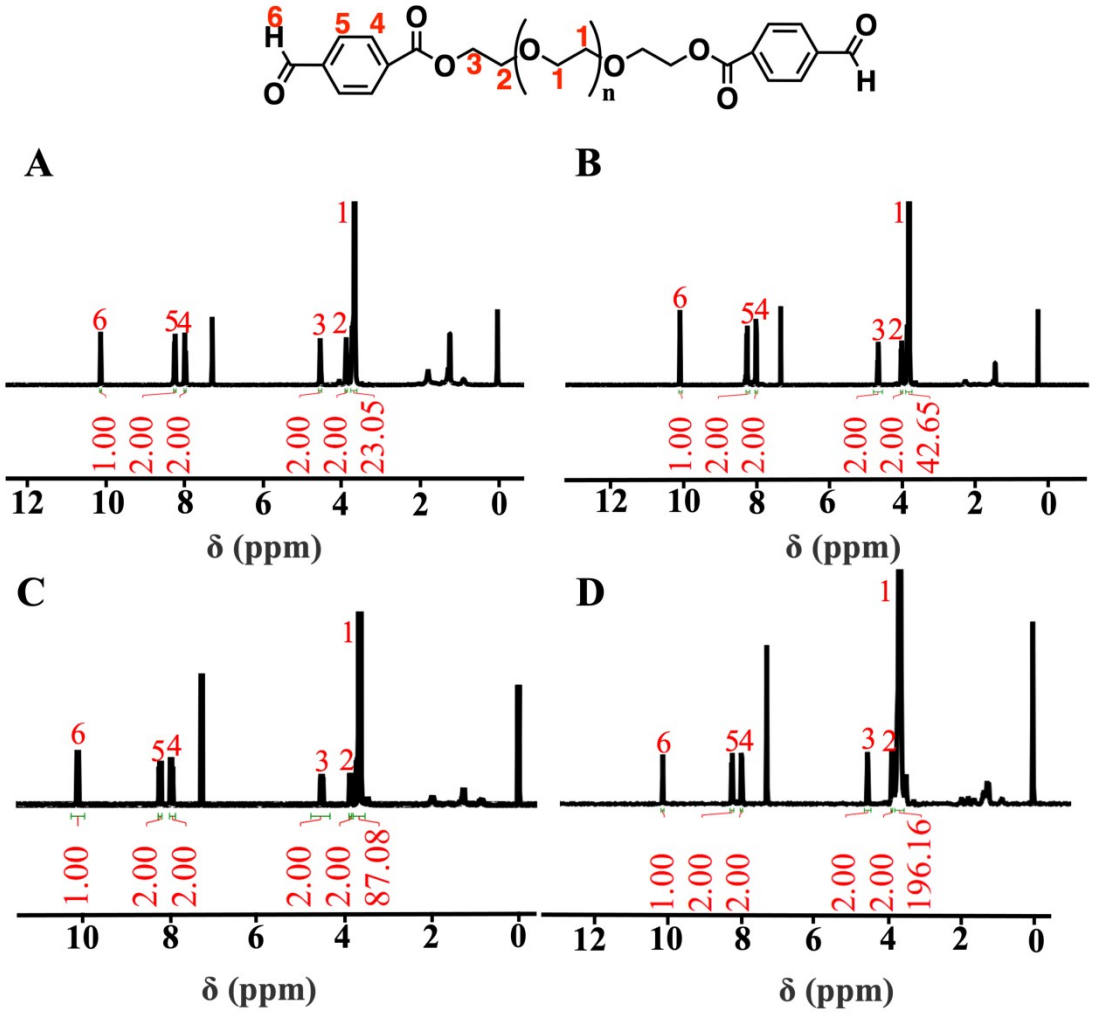


Figure S3. $^{1}H$ NMR spectra of CHO-PEG600-CHO (a), CHO-PEG1000-CHO (b), CHO-PEG2000-CHO (c), and CHO-PEG4000-CHO (d) in $CDCl_3$.

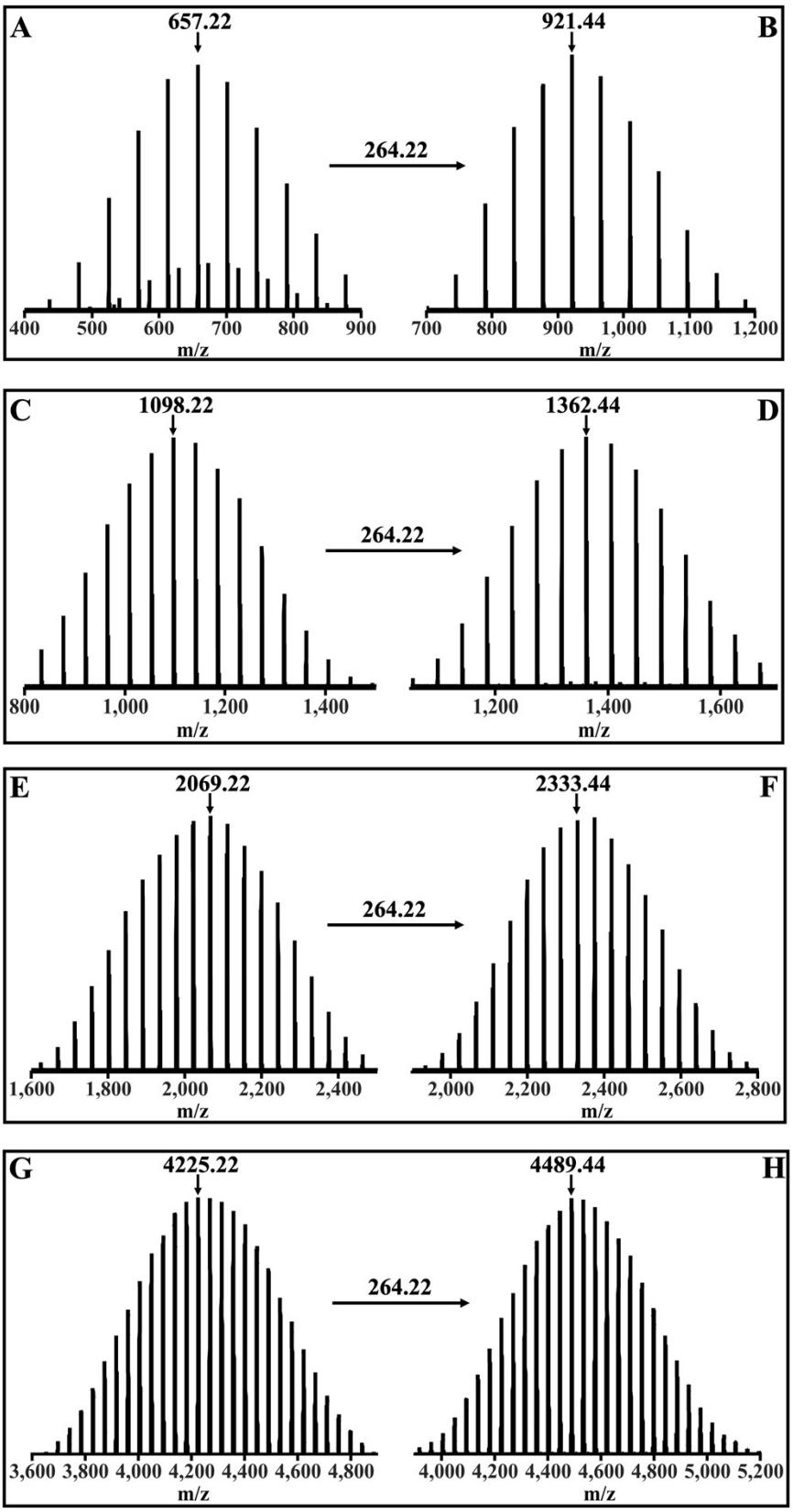


Figure S4. MALDI-TOF MS spectra of PEG600 (a), CHO-PEG600-CHO (b), PEG1000 (c), CHO-PEG1000-CHO (d), PEG2000 (e), CHO-PEG2000-CHO (f), PEG4000 (g), and CHO-PEG4000-CHO (h).

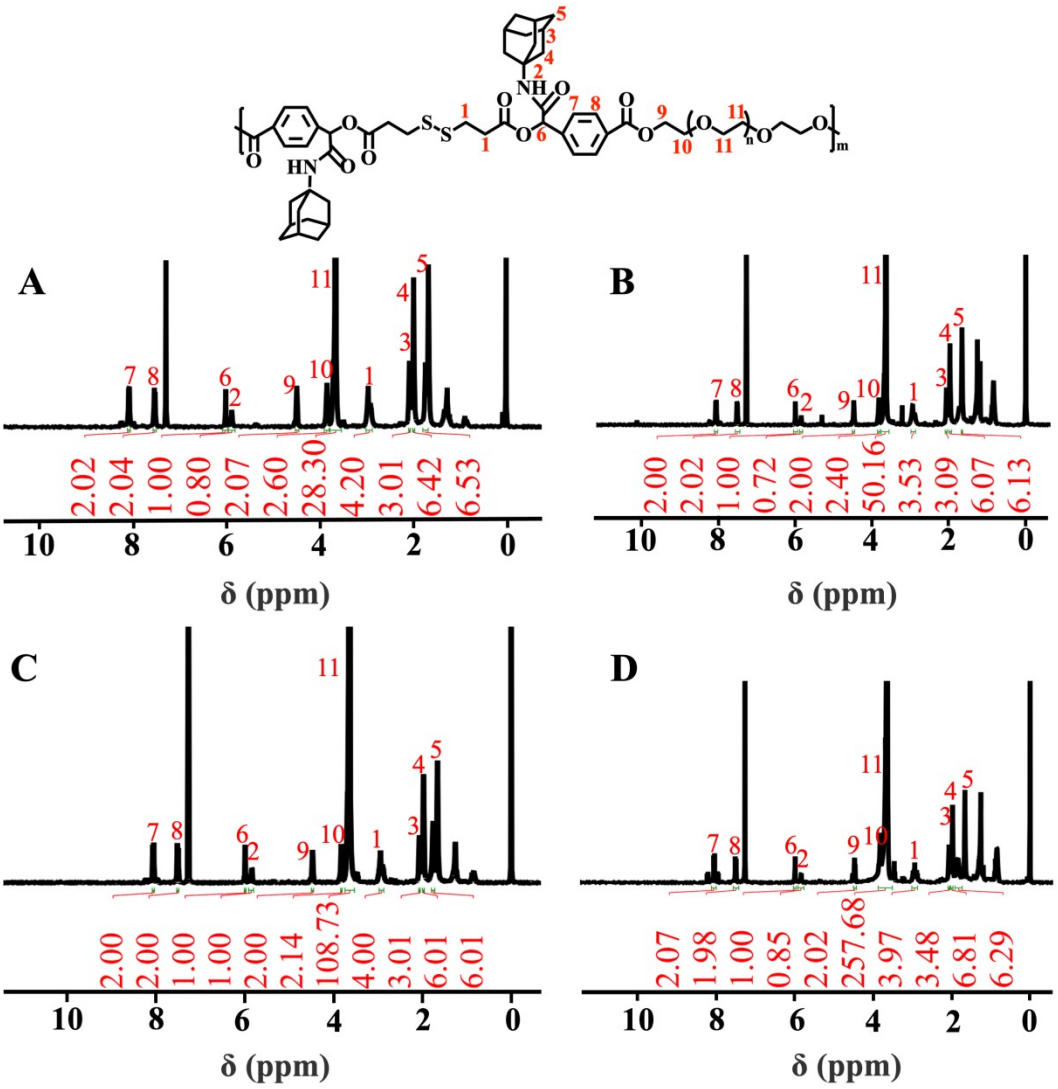


Figure S5. $^{1}H$ NMR spectra of P(PEG600) (a), P(PEG1000) (b), P(PEG2000) (c), and P(PEG4000) (d) in $CDCl_3$.

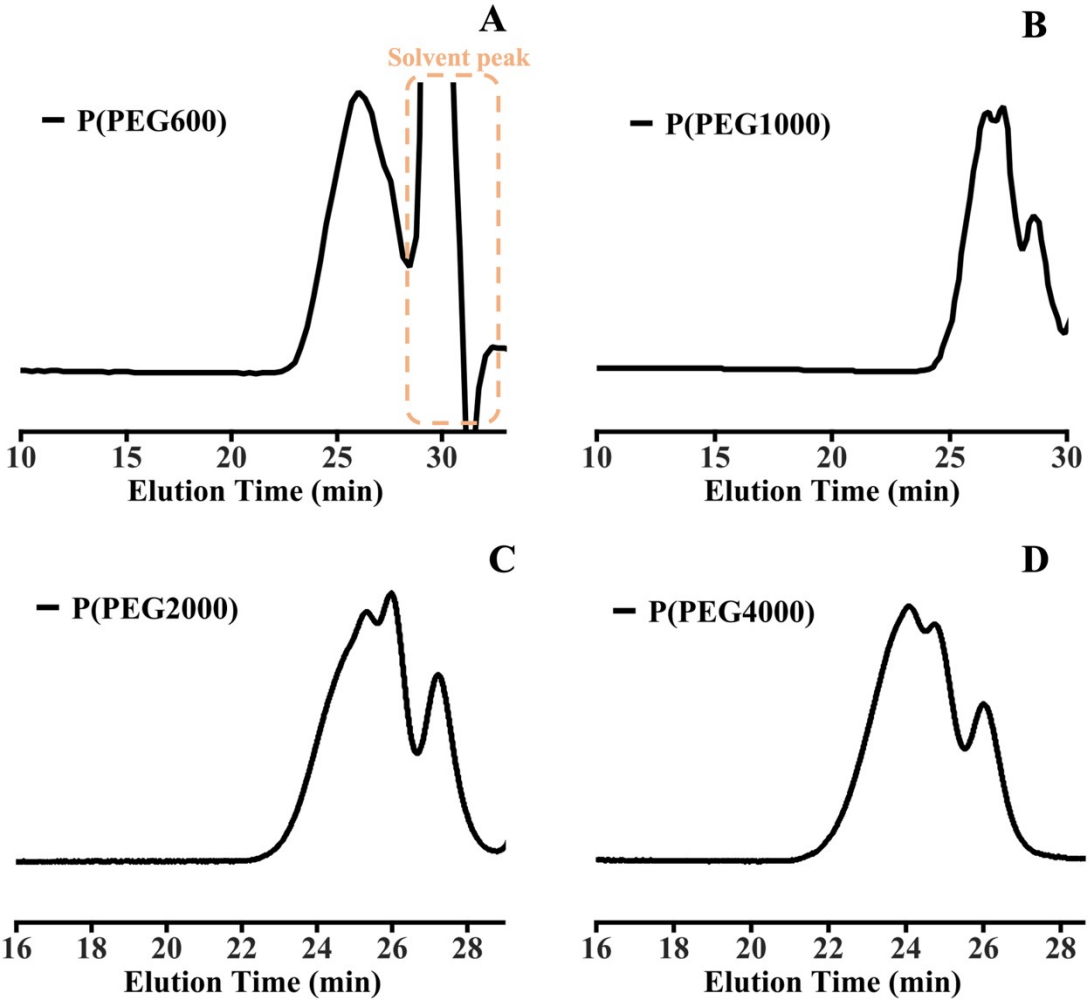


Figure S6. SEC curves of P(PEG600) (a), P(PEG1000) (b), P(PEG2000) (c), and P(PEG4000) (d).

Table S1. $M_n$ and dispersity of P(PEG).

| P(PEG) | $M_n$ (kDa) | Dispersity |
|---|---|---|
| P(PEG600) | 12.8 | 1.42 |
| P(PEG1000) | 10.0 | 1.34 |
| P(PEG1500) | 11.0 | 1.58 |
| P(PEG2000) | 14.6 | 1.32 |
| P(PEG4000) | 25.5 | 1.34 |

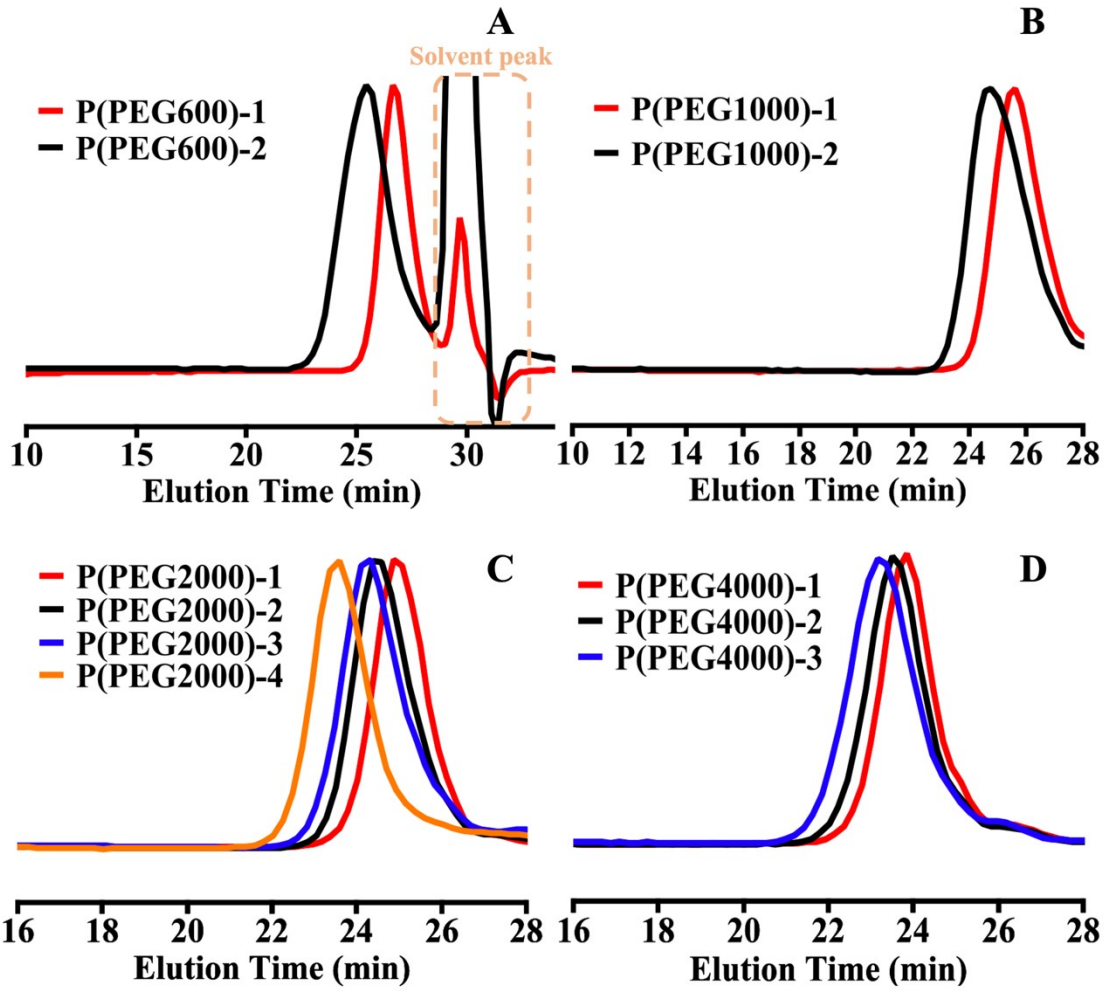


Figure S7. SEC curves of the fractions of P(PEG600) (a), P(PEG1000) (b), P(PEG2000) (c), and P(PEG4000) (d).

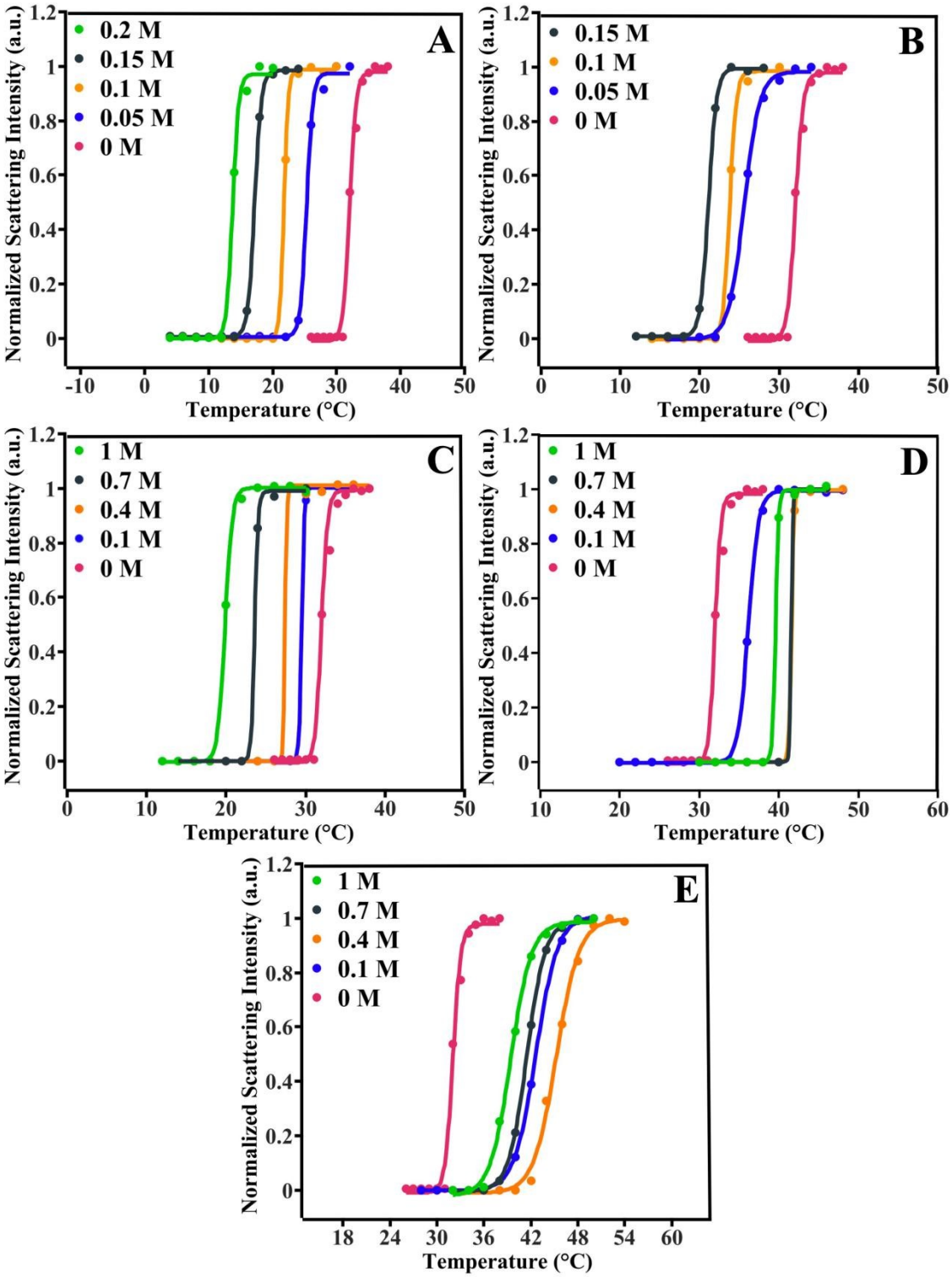


Figure S8. Temperature trends of the scattering intensities of P(PEG1500)-1 in $Na_2SO_4$ (a), $Na_2CO_3$ (b), NaCl (c), NaI (d), and NaSCN (e) solutions with different concentrations.

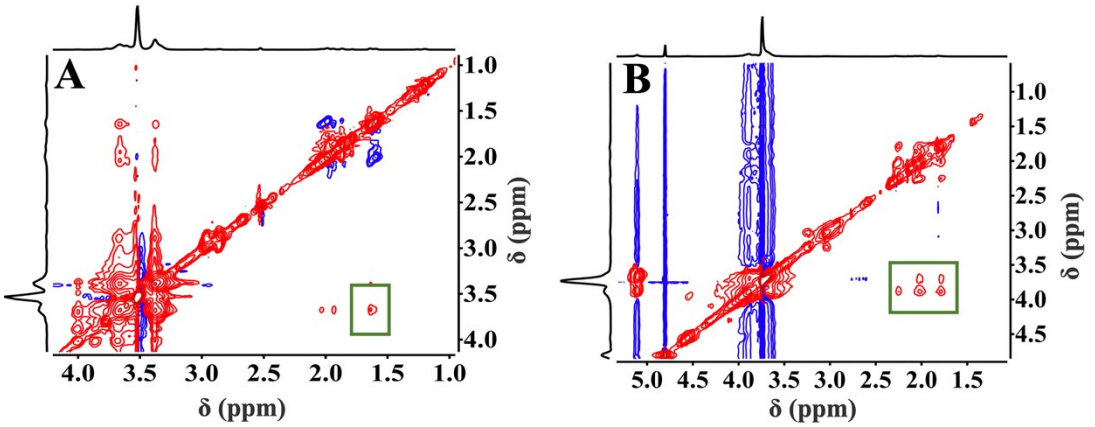


Figure S9. 2D $^{1}$H NOESY NMR spectra of P(PEG1000)-1/CD-$NH_2$ in DMSO (a) and P(PEG2000)-1/CD-$NH_2$ in $D_2O$ (b).

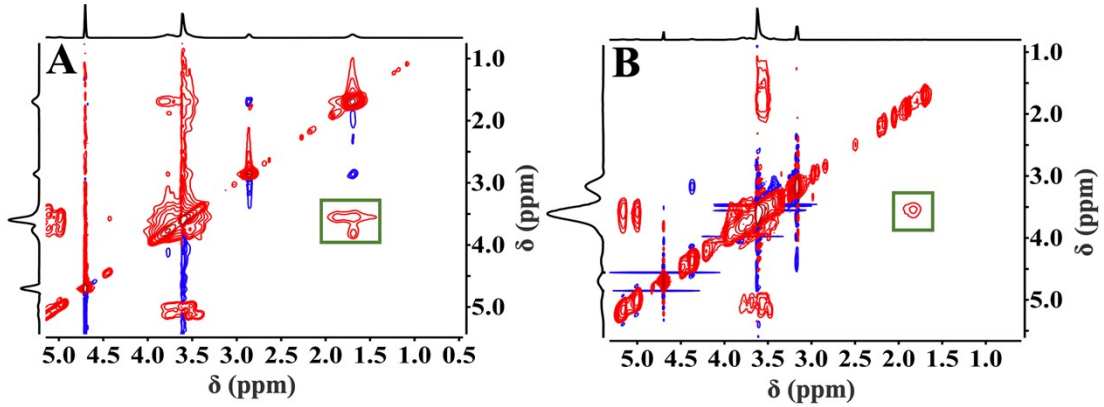


Figure S10. 2D $^{1}$H NOESY NMR spectra of P(PEG2000)-3 recognized with SBE-CD (a) and HTMAP-CD (b) in $D_2O$.

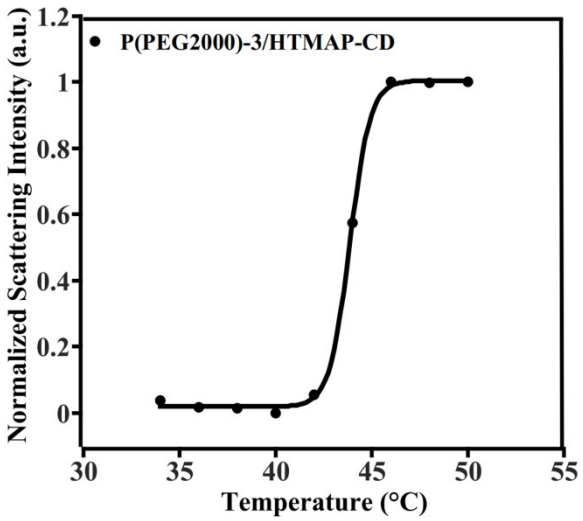


Figure S11. Temperature trend of the scattering intensities of the P(PEG2000)-3/HTMAP-CD in water.

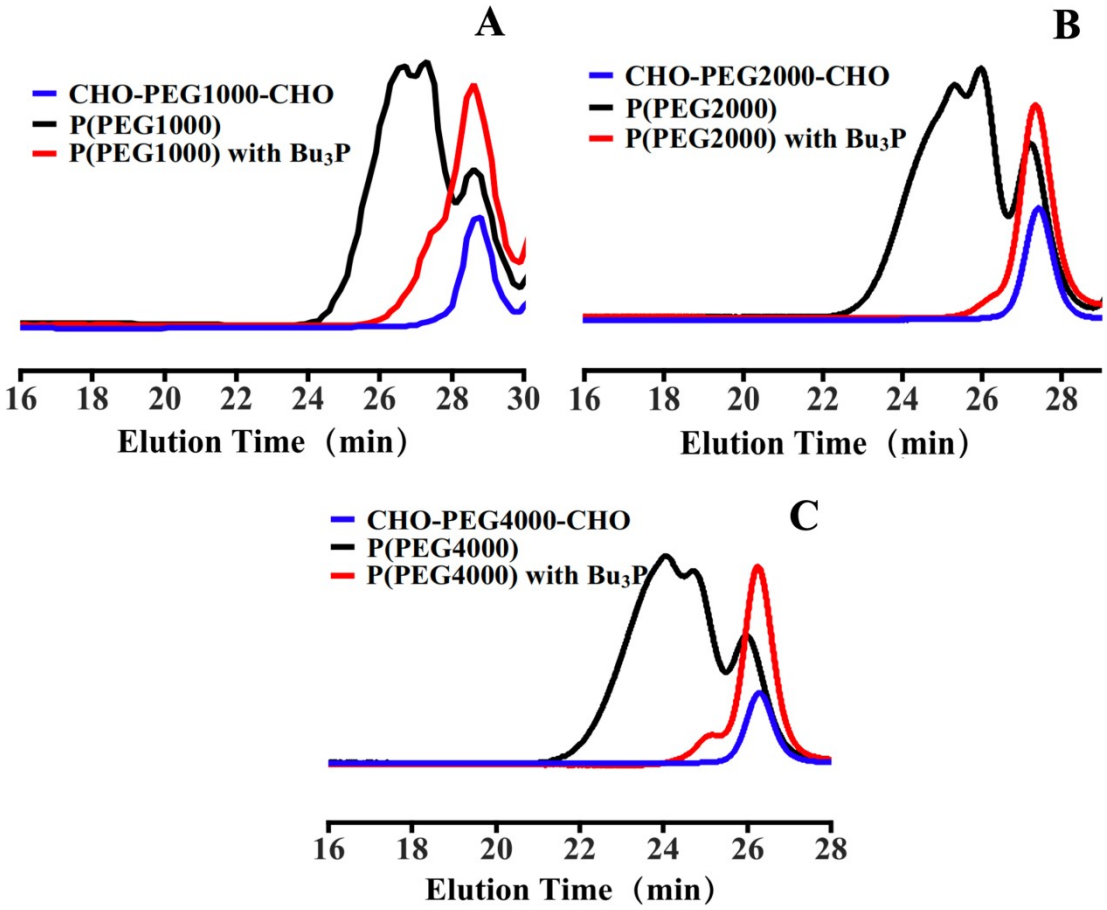


Figure S12. (a) SEC curves of CHO-PEG1000-CHO (blue line), P(PEG1000) (black line), and P(PEG1000) with $Bu_3P$ (red line) (b) SEC curves of CHO-PEG2000-CHO (blue line), P(PEG2000) (black line), and P(PEG2000) with $Bu_3P$ (red line) (c) SEC curves of CHO-PEG4000-CHO (blue line), P(PEG4000) (black line), and P(PEG4000) with $Bu_3P$ (red line) in DMF.

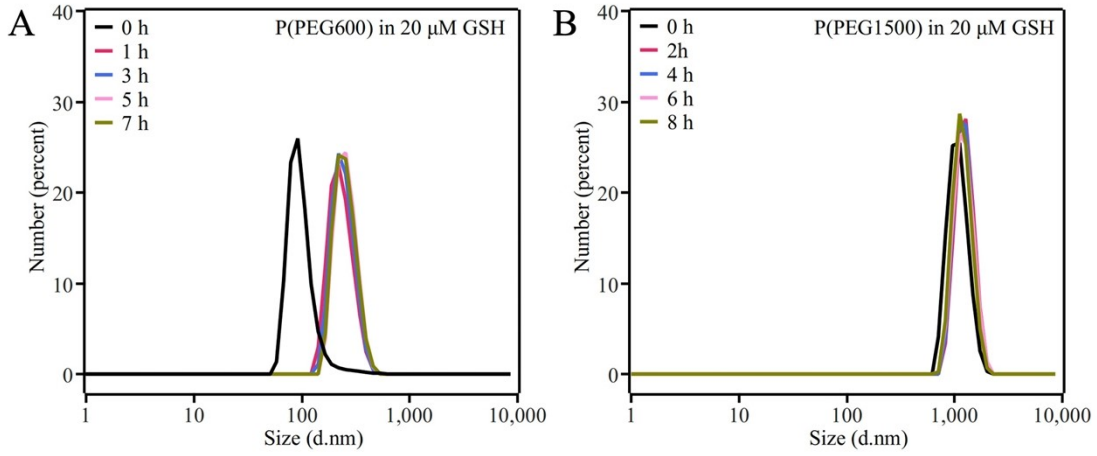


Figure S13. DLS results of P(PEG600)-1 (a) and P(PEG1500)-1 (b) degradation in 20 μM GSH solution.